Analytical Methods

Accepted Manuscript

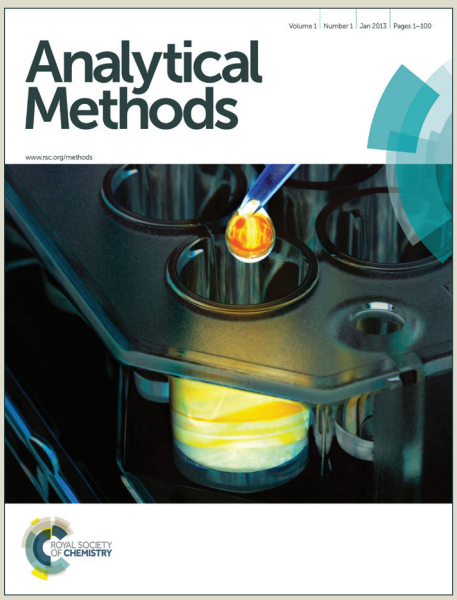

ROYAL SOCIETY OF CHEMISTRY

www.rsc.org/methods

Graphical Abstract- Synopsis

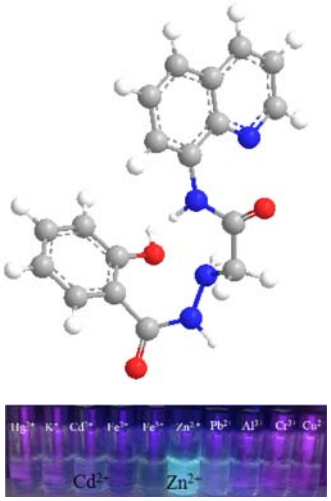

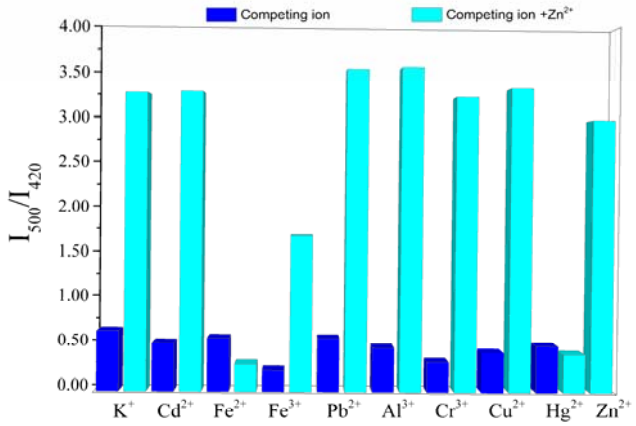

We report a ratiometric probe with 8-aminoquinoline as fluorophore and salicylhydrazide group as the receptor, which shows low detection limit for Zn^{2+}, and anti-interference towards Cd^{2+} and Pb^{2+}.

A Novel Ratiometric Fluorescence Sensor for Zn^{2+} Detection

Liqiang Gu, [a, b] Xuejuan Wan,[a, b, *] Haiyang Liu,[b] Tianqi Liu,[b] and Youwei Yao[b,**]

[a] Shenzhen Key Laboratory of Special Functional Materials, College of Materials Science and Engineering, Shenzhen University, Shenzhen 518060, PR China,

[b]Advanced Materials Institute, Graduate School at Shenzhen, Tsinghua University, Shenzhen 518055, PR China.

* Corresponding author. Tel: +86-0755-26534059, Fax: +86-0755-26534457

** Corresponding author. Tel: +86-0755-26036796, Fax: +86-0755-26036796

E-mail addresses: wanxj@szu.edu.cn (X. Wan), yaoyw@sz.tsinghua.edu.cn (Y. Yao)

ABSTRACT

A novel ratiometric fluorescent sensor for Zn^{2+}, 2-(2-(2-hydroxybenzoyl)hydrazinyl)-*N*-(quinolin-8-yl)acetamide (**F-1**) with quinoline as fluorophore and salicylhydrazide as receptor, was designed and synthesized. **F-1** shows high selectivity and sensitivity for Zn^{2+} over Cd^{2+} in methanol/tris-HCl (0.05 M) buffer solution (1:9, v/v, pH=7.0). Upon the addition of Zn^{2+}, an overall 5-fold increase in fluorescence emission ratio (I_{500}/I_{420}) was observed. An intermolecular charge transfer (ICT) mechanism is suggested for this ratiometric sensor.

KEYWORDS: ratiometric, fluorescent sensor, Zn^{2+}, intermolecular charge transfer.

As a relatively convenient method, fluorescence sensing of heavy and transition metal (HTM) ions has attracted considerable research attention on account of their excellent detection accuracy, fast response, operational simplicity, especially for real-time and online analysis.[1-6] However, this research still forefronts key challenges, such as selectivity and sensitivity of fluorescent probes for complex matrix or trace amount of targets.[7-10] Taking Zn^{2+} as an example, the fluorescent detection of Zn^{2+} is usually interfered by other HTM ions such as Cd^{2+}, Cu^{2+}, Hg^{2+}, Fe^{2+}, Co^{2+}, and Ni^{2+}.[11-15] In most reported literatures, the coordination mode between fluorescence sensor and Cd^{2+} was the same as Zn^{2+}, and similar fluorescence responds (intensity and/or wavelengths changes) can be obtained,[16-20] which made the testing results incredible. Developing highly selective Zn^{2+} sensor against the interference of Cd^{2+} ion has now drawn considerable research attention, and three main strategies was employed. The first one relies on the variation of the detection condition (solvent, buffer, pH).[21-25] Lu *et al*. have reported a ratiometric sensor, which can successfully discriminate Cd^{2+} and Zn^{2+} by two diverse internal charge transfer (ICT) processes.[26] However, the construction of these particular fluorescent sensors still possesses inherent limitations, as the discrimination mechanism between Zn^{2+} and Cd^{2+} is complicated and usually has no common rules to follow. Thus, relatively few cases have been reported. The second strategy utilized the different fluorescence signal output to discriminate Cd^{2+} and Zn^{2+} (different stokes shift).[27-31] For example, Tan *et al.* have reported a probe to distinguish Zn^{2+} and Cd^{2+} with high sensitivity and selectivity, which shows maximum fluorescence emission peaks at 455 nm after the addition of Cd^{2+}, but 495 nm after the addition of Zn^{2+}.[32] Under certain circumstances, the competing recognition process presented in one indicator could probably be a serious obstacle for the sensitive and selective detection of Zn^{2+} ion. The

third strategy involves the design of appropriate recognition site in the fluorescence sensor, which can only response to one specific analyte.[33-38] Considering the practical feasibility and the detection applicability, the last method obviously has great research potential.

It has been reported that probes with 8-aminoquinoline as fluorophore exhibited high recognition potential toward Zn^{2+}, ascribing to the pyridinic nitrogen existed in the probe.[36-38] Considering the strong electron-donating ability of the hydrazine group, we wondered if the salicylhydrazide-receptor can provide more coordination sites and additional water solubility in the fluorescence sensing process of Zn^{2+} (**F-1,** Scheme S1).

F-1 was synthesized from 8-aminoquinoline by two-steps, and its structure was confirmed by ^{1}H NMR, ^{13}C NMR, HR-MS and FT-IR. (Figure. S1-S4). ^{1}H NMR and ^{13}C NMR spectra of **F-1** are consistent with the assigned structure in Figure S1 and Figure S2. Figure S3 shows the FT-IR spectrum of **F-1**, where the characteristic peak of 1245 cm^{-1} (Ph—N); 1356 cm^{-1}(Ph—O); 1537 cm^{-1} (N—H bending) and 1644 cm^{-1} (C═O) demonstrate the existence of aminoquinoline group and salicylhydrazide group in **F-1**. In addition, the HR-MS result exhibit a group of peaks located at *m*/*z* 337.1314 ($[M+1]^{+}$), which further confirms the chemical structure of **F-1** (Figure S4).

The fluorescence detection selectivity of **F-1** was investigated, and the results were shown in Figure 1. **F-1** showed scarcely fluorescence emission change among the range of 350-680 nm in methanol/tris-HCl (0.05M) buffer solution (1:9, v/v, pH=7.0) after the addition of K^{+}, Cd^{2+}, Fe^{2+}, Fe^{3+}, Pb^{2+}, Al^{3+}, Cr^{3+} and Cu^{2+} ion. However, fluorescence intensity enhancement (I=9.48×10^{6}, $\lambda_{max(em)}$=500 nm) and a remarkable red-shift of 80 nm were observed for **F-1** in the presence of Zn^{2+} ion, which can be assigned to an internal charge transfer (ICT) in the excited state of **F-1**. Simultaneously, an obviously green-yellow emission of the solution can easily be visualized by naked eye under UV

lamp (365 nm, inset of Figure 1).

<Approximate locations of Figure 1>

ICT mechanism has been widely exploited for the cation fluorescence sensing.[39] After target cation has been recognized by the fluorescence probe, variation of the electron-donating ability of substitution in fluorogen could change emissive wavelengths effectively. If the electron-donating ability of the electron-rich group is reduced, blue shifts of both the absorption and fluorescence spectra are expected. Conversely, if the determinant promotes the electron-donating character of the corresponding group, red-shift of the fluorescence emission spectrum can be achieved. In the current situation, electron transfer from amide nitrogen adjacent to the quinoline fluorogen to Zn^{2+} enhances the ICT process of **F-1,** and a remarkable red-shift of 80 nm were observed.

To further explore the selectivity of **F-1** for Zn^{2+}, competition experiments were conducted in the presence of Zn^{2+} mixed with K^{+}, Cd^{2+}, Fe^{2+}, Fe^{3+}, Pb^{2+}, Al^{3+}, Cr^{3+}, Cu^{2+}, and Hg^{2+} ions, respectively. As shown in Figure 2, most of the metal cations especially Cd^{2+}, Pb^{2+} showed scarcely interference with the detection of Zn^{2+} ion, suggesting that probe F-1 possesses excellent application for Zn^{2+} detection under the fact that cadmium and lead are often associated in zinc ore. It should be noted that the probe exhibit relatively poor detection selectivity in the presence of Fe^{2+} and Hg^{2+}, and the tolerate limit (Figure S6) of the error-free detection of Zn^{2+} (10 μM) with F-1 (10 μM) was determined to 2.5 μM for Hg^{2+}, and 6 μM for Fe^{2+}, respectively. Considering that Fe^{2+} was unstable in natural environment and Hg^{2+} has relatively small solubility, F-1 still have the potential in practical sensing process. Moreover, the current probe can also be utilized with the other reported sensor which was not influenced by Fe^{2+} and Hg^{2+}, and the mutual complementation of the two sensors will achieve accurate Zn^{2+} detection in complex

environment. [40-41]

<Approximate locations of Figure. 2>

The UV-Vis and fluorescence titrations were carried out by gradual addition of various amounts of Zn^{2+}, respectively (Figure 3 and Figure 4). As **F-1** was dispersed in neutral methanol/water (v/v=1:9) solution buffered by 0.05M Tris-HCl, the UV-Vis absorption spectra of **F-1** exhibited multiple absorption band over 200~375 nm region. The addition of Zn^{2+} immediately resulted in a significant change of absorbance band in the ultraviolet range of 200-325 nm, and a new absorbance peak at 345 nm was observed. (Figure 3).

<Approximate locations of Figure 3>

Upon the gradual addition of Zn^{2+}, about 5-fold increase in fluorescence intensity at 500 nm and 80 nm red-shift from 420 to 500 nm of fluorescence emission are observed in Tris-HCl (0.05M, MeOH/H_2O=1:9, v/v, pH 7.0) buffer solution (Figure. 4a). A nearly linear relationship is obtained between the fluorescence intensity ratios at 500 nm and 420 nm (I_{500}/I_{420}) of sensor **F-1** at low concentration of Zn^{2+} (0-0.35 equiv, Figure 4b), where linearly dependent equation is y=1.0+0.6995x, linearly dependent coefficient is R^2=0.9982. The change of linearly relationship for **F-1** with the Zn^{2+} concentration can be explained in terms of the complex coordination structure, as there are many possible coordination sites for Zn^{2+} ion in **F-1**. The detection limit was then determined to 1.4×10^{-7} M from the equation DL = 3 Sb_1/S, where Sb_1 is the standard deviation of the blank solution and S is the slope of the calibration curve as literature reports.[42-44]

<Approximate locations of Figure 4>

Moreover, comparing with the mass spectrum, probe **F-1** with Zn^{2+} exhibit a cluster peak located at m/z 399.0433 (**F-1**+Zn^{2+}-H), which further indicates a 1:1 complex

between the probe and Zn^{2+} (Figure S4 and Figure S5).

The Zn^{2+}-sensing ability of **F-1** at different pH values was also investigated. As shown in Figure 5, **F-1** has no fluorescence response to Zn^{2+} in the acidic environment (pH < 5) due to the protonation of the amino group in **F-1,** leading to a weak coordination ability to Zn^{2+}. However, satisfactory Zn^{2+}-sensing abilities can be achieved when the pH increased from 6 to 10. At pH 7.0, the $I_{F\text{-}1+Zn(II)}/I_{F\text{-}1}$ value reaches its optimum point at 500 nm, but $I_{F\text{-}1}$ at 420 nm did not change too much, indicating that **F-1** possessed the highest sensing ability under the physiological pH window. Thus, all the fluorescence detection was conducted at pH 7.0.

<Approximate locations of Figure 5>

The fluorescence spectrum of probe **F-1** at different pH values is shown in Figure 6. When it was excited at 340 nm, the fluorescence intensities at 420 nm increased with increasing pH (6~10). A nearly linear relationship is obtained between the fluorescence intensity at 420 nm of **F-1** and pH at the range of 7.0~10.0 (Fig. 6(b), with a linearly dependent coefficient of R^2=0.9928).

<Approximate locations of Figure 6>

In conclusion, we have developed bi-functional fluorescent probe (**F-1)** for Zn^{2+} and pH based on aminoquinoline, with salicylhydrazide as receptor. The obtained fluorescence sensor can achieve highly sensitive and selective ratiometric Zn^{2+} sensing without the interference of Cd^{2+} and Pb^{2+} ions, which always accompanied with each other in zinc mineral-rich area.[45-46] As a ratiometric fluorescent probe, **F-1** can effectively eliminate the background interference and the fluctuation of detection conditions. Besides, **F-1** also shows a nearly linear fluorescence intensity enhancement at pH range of 7.0~10.0, suggesting that the current probe can also be utilized as a sensitive pH indicator at

relatively mild pH conditions.

Acknowledgment

The financial support from National Natural Scientific Foundation of China (NNSFC) Project (21204042), National High Technology Research and Development Program of China (863 Program, 2012AA030312), Fundamental Research Project of Shenzhen (JCYJ20120830152316443) and Technology Innovation Program of Shenzhen (CXZZ20130322101824104) are gratefully acknowledged.

References

1 Jiang, P.; Guo, Z. *Coordination Chemistry Reviews* **2004**, *248*, 205.

2 Bruchez, M.; Moronne, M.; Gin, P.; Weiss, S.; Alivisatos, A. P. *Science* **1998**, *281*, 2013.

3 Xu, Z.; Han, S. J.; Lee, C.; Yoon, J.; Spring, D. R. *Chemical Communications* **2010**, *46*, 1679.

4 Zhang, X.; Shiraishi, Y.; Hirai, T. *Tetrahedron letters* **2007**, *48*, 5455.

5 Xu, Z.; Qian, X.; Cui, J. *Organic letters* **2005**, *7*, 3029.

6 Burdette, S. C.; Walkup, G. K.; Spingler, B.; Tsien, R. Y.; Lippard, S. J. *Journal of the American Chemical Society* **2001**, *123*, 7831.

7 Descalzo, A. B.; Martínez-Máñez, R.; Radeglia, R.; Rurack, K.; Soto, J. *Journal of the American Chemical Society* **2003**, *125*, 3418.

8 Xiang, Y.; Tong, A.; Jin, P.; Ju, Y. *Organic Letters* **2006**, *8*, 2863.

9 Yang, R.-H.; Chan, W.-H.; Lee, A. W.; Xia, P.-F.; Zhang, H.-K.; Ke'An L i* *Journal of the American Chemical Society* **2003**, *125*, 2884.

10 Maruyama, S.; Kikuchi, K.; Hirano, T.; Urano, Y.; Nagano, T. *Journal of the American Chemical Society* **2002**, *124*, 10650.

11 He, C.; Zhu, W.; Xu, Y.; Zhong, Y.; Zhou, J.; Qian, X. *Journal of Materials Chemistry* **2010**, *20*, 10755.

12 Nolan, E. M.; Lippard, S. J. *Accounts of chemical research* **2008**, *42*, 193.

13 Li, N.; Xiang, Y.; Chen, X.; Tong, A. *Talanta* **2009**, *79*, 327.

14 Hagimori, M.; Mizuyama, N.; Yamaguchi, Y.; Saji, H.; Tominaga, Y. *Talanta* **2011**, *83*, 1730.

15 Komatsu, K.; Urano, Y.; Kojima, H.; Nagano, T. *Journal of the American Chemical Society* **2007**, *129*, 13447.
16 Liu, Z.; Zhang, C.; Li, Y.; Wu, Z.; Qian, F.; Yang, X.; He, W.; Gao, X.; Guo, Z. *Organic letters* **2009**, *11*, 795.
17 Ngwendson, J. N.; Banerjee, A. *Tetrahedron Letters* **2007**, *48*, 7316.
18 Meng, X. M.; Zhu, M. Z.; Liu, L.; Guo, Q. X. *Tetrahedron letters* **2006**, *47*, 1559.
19 Shiraishi, Y.; Ichimura, C.; Hirai, T. *Tetrahedron Letters* **2007**, *48*, 7769.
20 Hennrich, G.; Sonnenschein, H.; Resch-Genger, U. *Journal of the American Chemical Society* **1999**, *121*, 5073.
21 Wan, X.; Yao, S.; Liu, H.; Yao, Y. *Journal of Materials Chemistry A* **2013**, *1*, 10505.
22 Atilgan, S.; Ozdemir, T.; Akkaya, E. U. *Organic Letters* **2008**, *10*, 4065.
23 Xue, L.; Liu, Q.; Jiang, H. *Organic Letters* **2009**, *11*, 3454.
24 Du, P.; Lippard, S. J. *Inorganic chemistry* **2010**, *49*, 10753.
25 Chen, H. L.; Guo, Z. F.; Lu, Z. l. *Organic Letters* **2012**, *14*, 5070.
26 Lu, C.; Xu, Z.; Cui, J.; Zhang, R.; Qian, X. *The Journal of organic chemistry*, **2007**, *72*, 3554.
27 Xue L.; Liu Q.; Jiang H. *Organic letters*, **2009**, *11*, 3454.
28 Xu Z.; Baek K. H.; Kim H. N.; *et al*. *Journal of the American Chemical Society*, **2009**, *132*, 601.
29 Wilson E. M. *Journal of Biological Chemistry*, **1985**, *260*, 8683.
30 Jana S.; Dalapati S.; Alam M. A.; *et al*. *Journal of Photochemistry and Photobiology A: Chemistry*, **2012**, *238*, 7.
31 Pal, P.; Rastogi, S. K.; Gibson, C. M.; Aston, D. E.; Branen, A. L.; Bitterwolf, T. E. *ACS applied materials & interfaces* **2011**, *3*, 279.
32 Tan Y.; Gao J.; Yu J.; et al. *Dalton Transactions*, **2013**, *42*, 11465.
33 Zhang, Y.; Guo, X.; Jia, L.; Xu, S.; Xu, Z.; Zheng, L.; Qian, X. *Dalton Transactions* **2012**, *41*, 11776.
34 Zhang, L.; Cui, X.; Sun, J.; Wang, Y.; Li, W.; Fang, J. *Bioorganic & medicinal chemistry letters* **2013**, *23*, 3511.
35 Kim, J. H.; Hwang, I. H.; Jang, S. P.; Kang, J.; Kim, S.; Noh, I.; Kim, Y.; Kim, C.; Harrison, R. G. *Dalton Trans.* **2013**, *42*, 5500.
36 Zhang, Y.; Guo, X.; Si, W.; Jia, L.; Qian, X. *Organic letters* **2008**, *10*, 473.
37 Zhang, L.; Duan, D.; Cui, X.; Sun, J.; Fang, J. *Tetrahedron.* **2013**, *69*, 15.
38 Pal, P.; Rastogi, S. K.; Gibson, C. M.; Aston, D. E.; Branen, A. L.; Bitterwolf, T. E. *ACS Applied Materials & Interfaces.* **2011**, *3*, 279.

39 Hou, J.; Chen, H. Y.; Zhang, S.; Li, G.; Yang, Y. *Journal of the American Chemical Society*. **2008**, *130*, 16144.

40 Mourzina, Y. G.; Schubert, J.; Zander, W.; Legin, A.; Vlasov, Y. G.; Lüth, H.; Schöning, M. J. *Electrochimica Acta*, **2001**, *47*, 251.

41 Lee, J. W.; Jung, H. S.; Kwon, P. S.; Kim, J. W.; Bartsch, R. A.; Kim, Y.; Kim, J. S. *Organic letters*, **2008**, 10, 3801.

42 Barba-Bon, A.; Costero, A. M.; Gil, S.; Parra, M.; Soto, J.; Martínez-Máñez, R.; Sancenón, F. *Chemical Communications*. **2012**, *48*, 3000.

43 Zhang, J.; Zhou, Y.; Hu, W.; Zhang, L.; Huang, Q.; Ma, T. *Sensors and Actuators B: Chemical*, **2013**, *183*, 290.

44 Liu, S. R.; Wu, S. P. Sensors and Actuators B: Chemical, **2012**, *171*, 1110.

45 Nawar, N.; Ebrahim, M.; Sami, E. *Academic Journal of Interdisciplinary Studies*. **2013**, *2*, 85.

46 Du, A. X.; Cao, L. X.; Zhang, R. D. *Chin J Appl Environ Biol*, **2008**, 14, 650-653.

Figure Captions

Figure 1. Fluorescence spectra of **F-1** (10 μM) in tris-HCl (0.05 M) solution (methanol/water =1:9, v/v, pH=7.0) in the presence of different metal ions (5 equiv.) (λ_{ex}=340 nm). (Inset) Optical photographs (UV 365 nm) obtained for **F-1** after the addition of different metal ions (5 equiv.) (From left to right: Hg^{2+}, K^{+}, Cd^{2+}, Fe^{2+}, Fe^{3+}, Zn^{2+}, Pb^{2+}, Al^{3+}, Cr^{3+}, and Cu^{2+}).

Figure 2. Change of fluorescence intensity of **F-1** (10 μM) in various mixtures of metal ions (5 equiv. for each of the metal ions. (1) K^{+}+Zn^{2+}; (2) Cd^{2+}+Zn^{2+}; (3) Fe^{2+}+ Zn^{2+} (4) Fe^{3+}+ Zn^{2+}; (5) Pb^{2+}+Zn^{2+}; (6) Al^{3+}+Zn^{2+}; (7) Cr^{3+}+Zn^{2+}; (8) Cu^{2+} +Zn^{2+}; (9) Hg^{2+} +Zn^{2+}; (10)Zn^{2+}.

Figure 3. UV-vis absorption spectra of **F-1** (10 μM) in tris-HCl (0.05 M) solution (methanol/water =1:9, v/v, pH=7.0) with increasing Zn^{2+} concentration (0~2.0 equiv). (Inset) UV-vis absorption calibration curve at 214, 252 and 345 nm as a function of Zn^{2+} concentration.

Figure 4. (a) Fluorescence spectra for **F-1** (10 μM) in tris-HCl (0.05M) solution (methanol/water =1:9, v/v, pH=7.0) with increasing Zn^{2+} concentration (0~3.0 equiv). (λ_{ex} =340 nm, λ_{em1}=420 nm, λ_{em2}=500 nm) (Inset) Ratiometric calibration curve I_{500} /I_{420} as a function of Zn^{2+} concentration. (b) Variation of relative fluorescence intensity (I_{500}) for **F-1** (10 μM) in the presence of Zn^{2+} (0~0.35 equiv.)

Figure 5. Titration curve I_{500} nm of **F-1** (5 μM) at various pH values in methanol/water

(1:9, v/v) solution in the absence and presence of Zn^{2+} (1 equiv). (λ_{ex} =340 nm, λ_{em}=500 nm)

Figure 6. (a) Fluorescence intensity changes obtained for **F-1** (5 μM) at various pH values in methanol/water (1:9, v/v) solution. (λ_{ex} =340 nm, λ_{em}=420 nm) (Inset) Fluorescence intensity calibration curve I_{420} as a function of pH. (b) Variation of relative fluorescence intensity (I_{420}) for **F-1** (10 μM) at pH range of 7.0~10.0.

Figures

A Novel Ratiometric Fluorescence Sensor for Zn^{2+} Detection

Liqiang Gu, [a, b,] Xuejuan Wan,[a, b, *] Haiyang Liu,[b] Tianqi Liu,[b] and Youwei Yao[b,**]

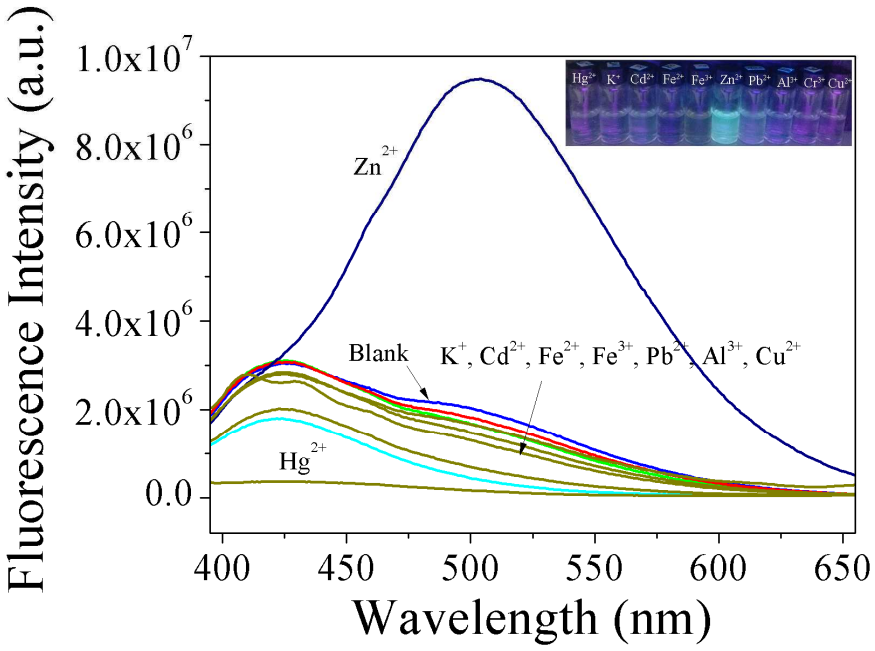

Figure 1

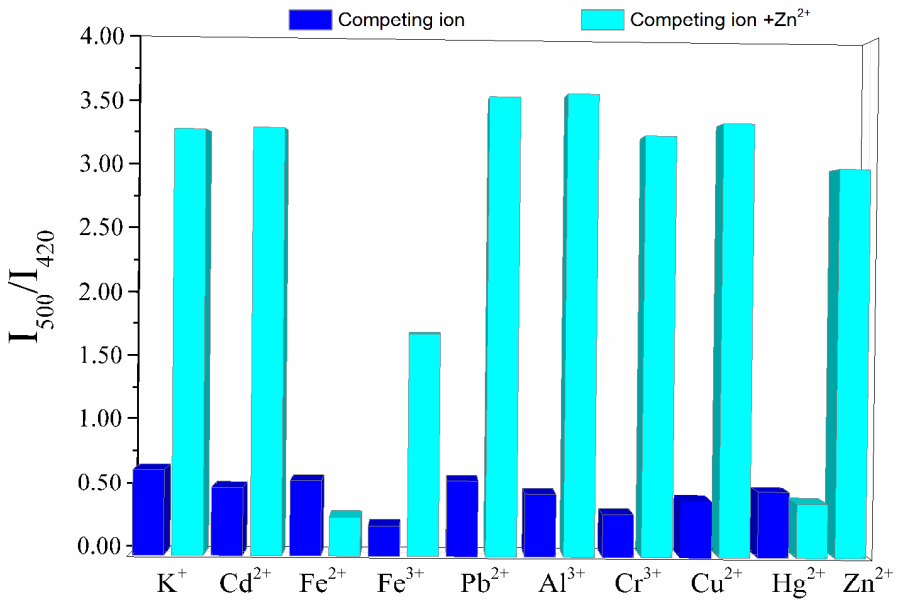

Figure 2

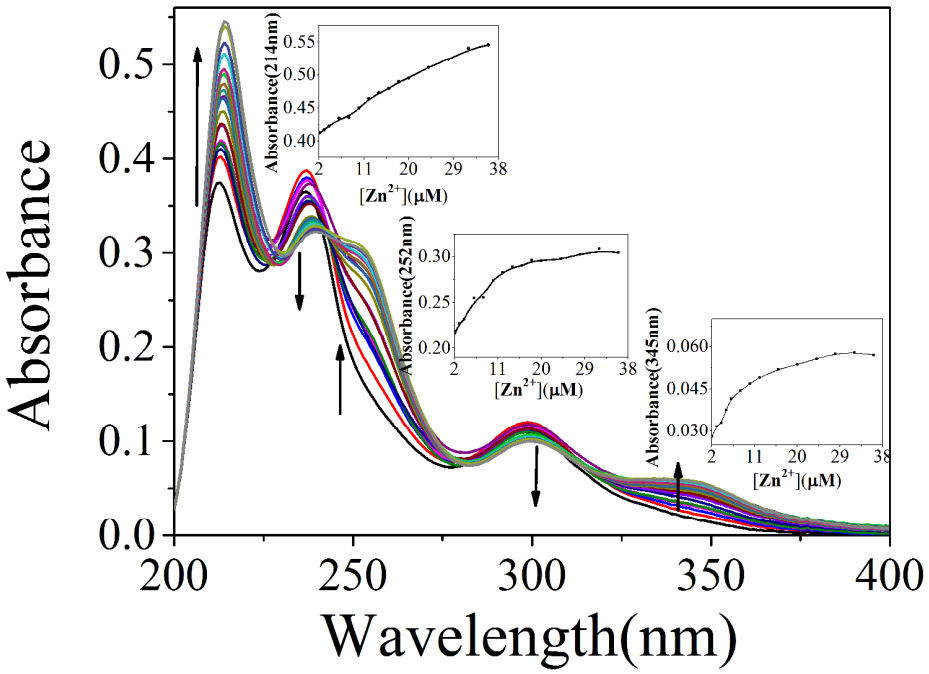

Figure 3

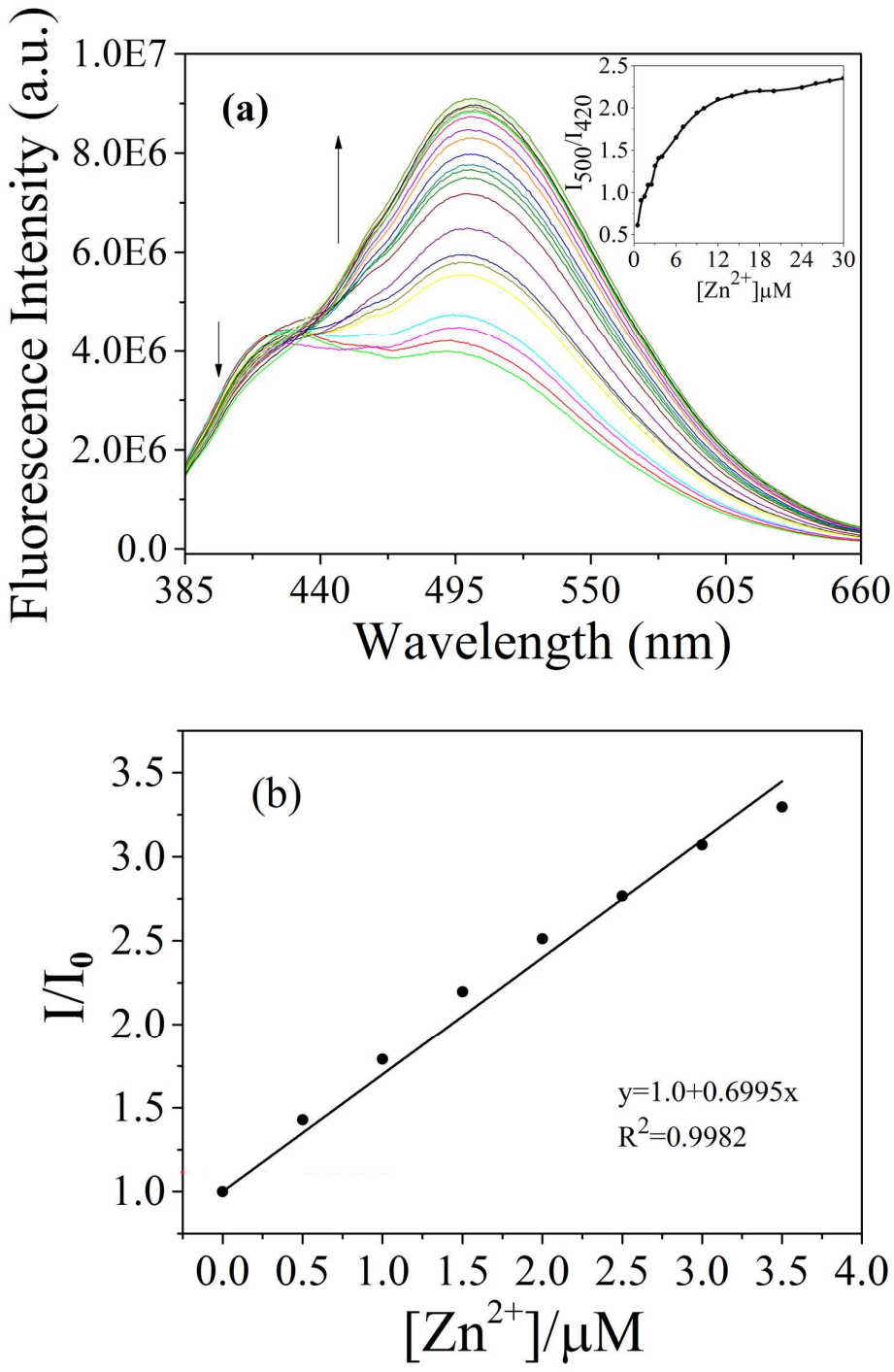

Figure 4

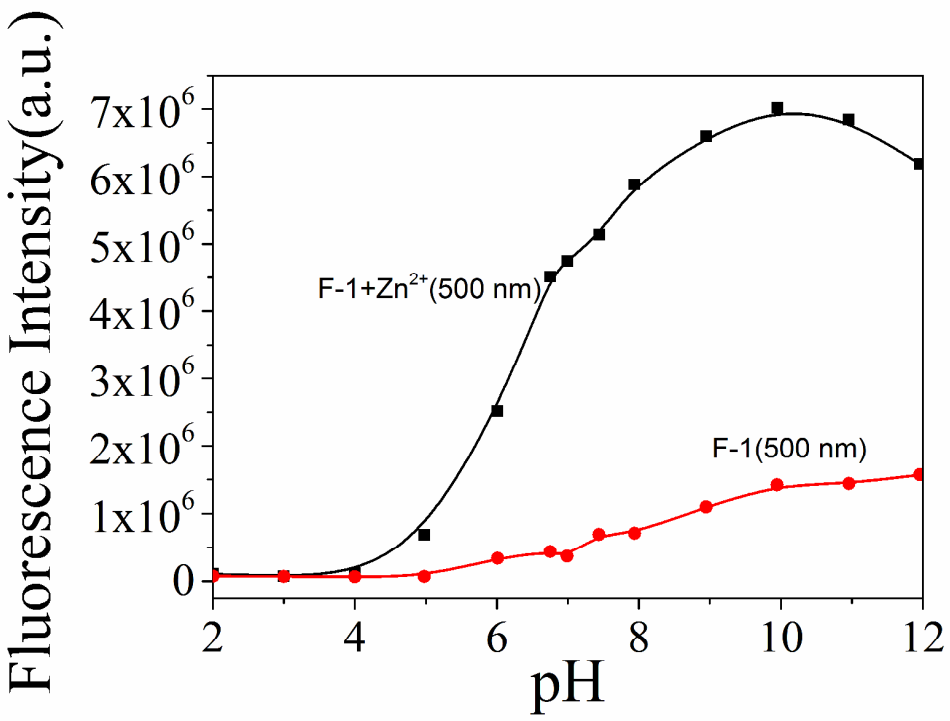

Figure 5

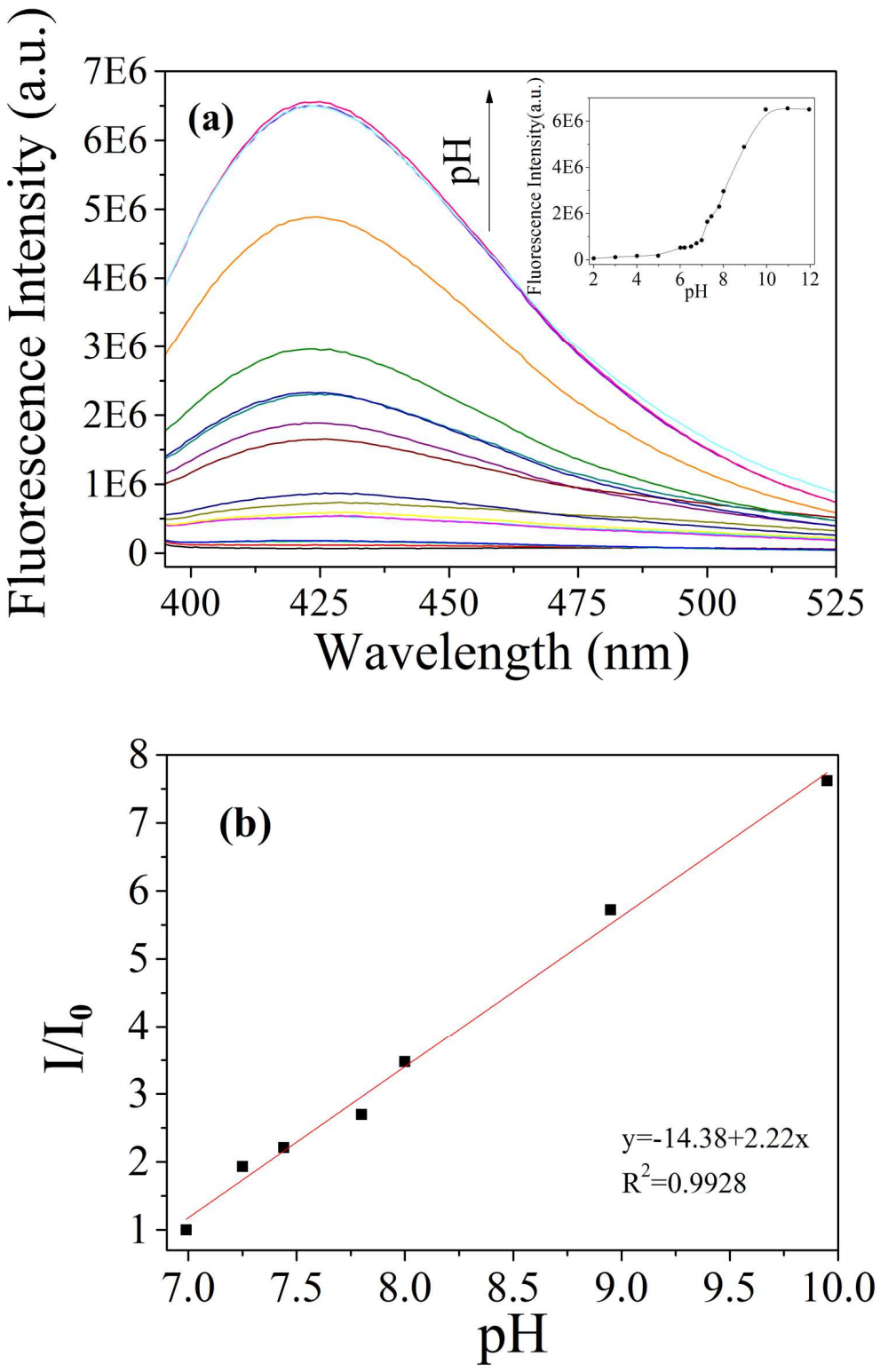

Figure 6